Filter Look Up Table method for Power Amplifiers Linearization

P. Jardin, G.Baudoin, *Member, IEEE ESIEE*

***Abstract*— This paper presents a new method of digital adaptive predistortion for linearization of Power Amplifiers (PA) exhibiting memory effects. The predistorter (PD) device consists of a Look-Up-Table (LUT) gain followed by a codebook of filters addressed by the index of the LUT. The adaptation is derived from direct learning for the LUT gains and indirect learning for the filter coefficients.**

We compared our results with those of two reference methods: a simple LUT system (with direct learning) and a memory polynomial system (with indirect learning).

The performances of the new approach lie between those of the two reference methods in terms of Adjacent Channel Power Regrowth and Error Vector Magnitude. The LUT is the less complex of the three methods but it is a memoryless system and it cannot correct the memory effects in the power amplifier. The memory polynomial PD is the more powerful but its complexity is very high. The new technique, due to the addition of filters to the LUT, has possibilities to compensate not only for the non-linearity but also for the memory effects in the PA and it is one order of magnitude less complex than the memory polynomial system.

***Index Terms*—baseband predistortion, linearization, non-linear distortions, power amplifier.**

I. Introduction

Power Amplifiers (PA) are critical elements of mobile communication systems because their efficiency conditions the autonomy and the weight of mobile handset batteries and their linearity influences on performance of the communication. An ideal PA is a perfectly linear device until a certain saturation output power P_{sat}^{out}. The output signal at a given instant is proportional to the input signal at the same instant as long as the input power is smaller than the input saturation power P_{sat}^{in}. In practice, PA are not perfectly linear and present memory effects, i.e. the output signal is a function of the current and of the previous input signal values. For common PA, the non-linearity effects and efficiency increase as the maximal input power $P_{\max}^{in}$ gets closer to its saturation value P_{sat}^{in}. A compromise must be achieved between the efficiency and the linearity of the PA [1].

The PA non-linearity generates amplitude and phase distortions on the PA output signal. These distortions create spectral regrowth in adjacent channels and deform the signal constellation, all the more since the dynamic of the input amplitude grows.

The use of constant-envelope modulations such as in the GSM system alleviates this problem. Yet, in order to increase the capacity and performances of wireless communications, new systems implement multilevel or multicarrier modulations and spread-spectrum techniques leading to signals with high Peak-to-Average Power Ratio (PAPR). To maintain an acceptable level linearity it is possible to operate the PA with a large backoff but this would be detrimental to the efficiency. Therefore, PA linearization is becoming an essential component of the communication system allowing a better compromise between linearity and efficiency. Moreover, with increasing bandwidth and average power of signals, PA memory effects cannot be ignored and PA linearization system should also compensate for these effects. These memory effects may be explained by frequency dependence of components or by thermal phenomena [2].

Many linearization techniques have been proposed [3] and among them digital baseband predistortion is one of the most effective. The principle of predistortion is to distort the PA input signal by an additional device called a predistorter (PD) whose characteristics are the inverse of those of the amplifier. For baseband predistortion systems, the transmission path includes the digital baseband PD, digital-to–analog converters (DAC), up-converters and the PA. In adaptive PD systems, it is necessary to add a feedback path consisting of a demodulator, analog-to-digital converters (ADC) and baseband PD adaptation. The schematic of an adaptive baseband PD system is shown in Fig. 1.

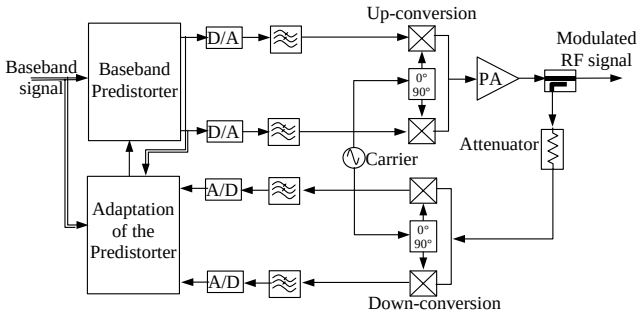

Fig. 1. Schematic of an adaptive baseband predistortion system

Manuscript received October 2003. The authors are with the ESYCOM Communication Systems laboratory and with the ESIEE, 2 Bd Blaise Pascal, BP 99, 93162, Noisy Le Grand, cedex, France (email: p.jardin@esiee.fr and g.baudoin@esiee.fr).

For more than fifteen years, there has been intensive research on predistortion techniques for memoryless PA. The predistortion function is commonly realized with a Look-up-Table (LUT). The LUT-based predistorters may be further classified as mapping PD [4], [5], polar PD [6]-[7] or gain based PD [8]-[9]. The PD function can also be implemented as a nonlinear function such as polynomial approximation of the ideal linearizer [10]-[11]. More recently, solutions have been proposed which address the problem of compensating both non linearity and memory effects in PA [12]-[25].

The digital baseband predistortion method presented here brings a new solution to this problem.

The first step of some of the existing digital baseband approaches is the identification of a PA model. This is not the case in our work, where we identify directly a model for the inverse of the PA. Moreover, most of the proposed models used as memory predistortion devices are based on Volterra series [17]-[18], Wiener-Hammerstein models [19]-[20], memory polynomials [12]-[16], or neural networks [21]. Although these models rely on rigorous mathematical bases and lead to accurate results they require quite complex adaptation techniques. We have devised a new model for the predistortion device which is based on the association of a Look Up Table (LUT) technique, which is widely used for memoryless PA, and FIR filters to take into account the memory effects. Compared to the approaches previously proposed, this method has the great advantage of simplicity and is easier to implement in real time systems.

In this paper, we first report (section II) some generalities on baseband predistortion systems and their learning structures. Then we present (section III) the new memory non-linear predistortion model, the Filter Look Up Table (FLUT) predistorter, and its adaptation with both direct and indirect learning. In a third part (section IV) we test this method on CDMA signals, determine an optimal set of parameters for the proposed PD and compare its performances and complexity with two other systems, namely a LUT (with direct learning) and a memory polynomial (with indirect learning). We complete this study by the analysis of the other impairments in the overall PD system (Fig.1) and conclude (section V).

II. ADAPTIVE BASEBAND PREDISTORTION SYSTEMS

A. *Baseband predistortion and operating point*

In this section, we use the formal frame of equivalent baseband models

If z is the (lowpass filtered) complex envelope of the PA input signal, the purpose of baseband predistortion is to find a baseband operator $\mathcal{F}$ such that:

$$\mathcal{A}\left(\mathcal{F}\left(z\right)\right) = G_0 z \,. \tag{1}$$

In this equation, $\mathcal{A}$ denotes the equivalent baseband operator for the PA and G_0 is the reference gain, i.e. the gain of the linearized PA.

As it is quite difficult to linearize the PA up to its saturated output power P_{sat}^{out}, the designer of the system restricts the amplitude range over which the linearization is applied. This range is characterized by the maximum desired output power $P_{\max}^{out}$ which is a fraction S of the saturation power: $P_{\max}^{out} = S P_{sat}^{out}$, where $0<S<1$. The span S is related to the peak backoff (PBO) by:

$$PBO = -10\log_{10}\left(S\right) \tag{2}$$

We denote $P_{\max}^{in}$, the input power corresponding to the maximum output power.

The output backoff (OBO) in dB is defined by:

$$OBO = 10\log_{10}\left(P_{sat}^{out}\right) - 10\log_{10}\left(\bar{P}\right), \tag{3}$$

where $\bar{P}$ is the average output power.

It is related to the PBO and peak to average power ratio (PAPR) by:

$$OBO = PBO + PAPR \,. \tag{4}$$

As large OBO values imply inefficient operation, it is advisable to work with small PBO ($S > 0.9$) and if necessary to reduce the PAPR by clipping the input signal, thus increasing distortion. There is then a tradeoff between PA efficiency and distortion level either with or without predistortion. The choice of the operating point is a crucial question which will be further discussed in section IV.A.2)b) .

B. *Direct or indirect learning structure*

We call "direct learning" of the PD the determination of its characteristics using the "direct" scheme (see Fig. 2.a).

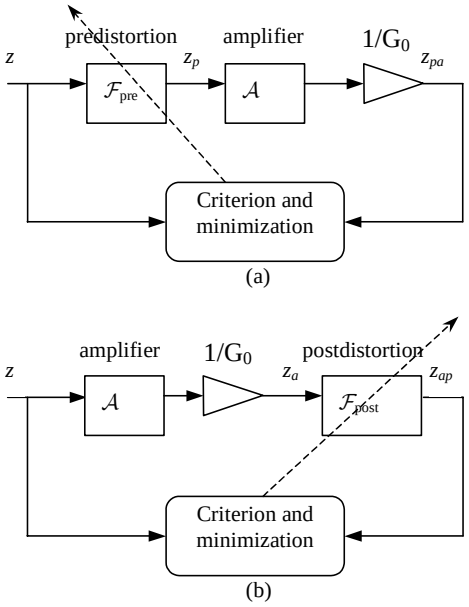

Fig. 2. Direct learning (a) and Indirect Learning (b) of predistortion

In this and the other figures, the complex envelop signals are differentiated by indices according to the following rule: the order of indices indicates the successive systems encountered by $z(n)$. For instance $z_{pa}(n)$ denotes the output of the cascade of the ***p***redistorter and the ***a***mplifier (divide by G_0). Also, the dashed line indicates the adaptation process.

In the direct learning approach, the ideal predistortion operator $\mathcal{F}_{\text{pre}}$ minimizes the error z_{pa}–z and is given by:

$$\mathcal{F}_{\text{pre}}(z) = \mathcal{A}^{-1}(G_0 z). \quad (5)$$

As $\mathcal{A}$ is a non-linear function, this ideal solution cannot be written explicitly from the observations z and z_{pa}.

In the indirect learning approach, we consider the fictive problem of postdistortion (see Fig.2.b). The ideal postdistortion operator $\mathcal{F}_{\text{post}}$ which minimizes the error z_{ap}–z is given by:

$$\mathcal{F}_{\text{post}}(z_a) = z. \quad (6)$$

This equation gives an explicit form for the postdistorter from the observations z_a and z.

As $z = \mathcal{A}^{-1}(G_0 z_a)$ (6) can also be written:

$$\mathcal{F}_{\text{post}}(z_a) = \mathcal{A}^{-1}(G_0 z_a) \quad (7)$$

From (5) and (7) we can conclude that both operators are identical.

In an indirect learning structure, a postdistortion system is computed and applied as a predistortion system. It has been demonstrated that this indirect approach is much more efficient than a direct one for predistortion systems like polynomials or Volterra models [11]-[20].

III. Proposed approach

A. LUT-FIR structure of the FLUT predistortion device

We propose an original form of predistorter for the compensation of PA non-linearity and memory effects. The predistorter itself presents both non-linearity and memory characteristics. As the memoryless non-linearity of the PD can be efficiently implemented by a Look-Up-Table (LUT) [4]-[9] and the memory can be represented by a filter, we consider a predistorter made of a LUT followed by a codebook of filters (one filter for each entry of the LUT). The overall predistortion system $\mathcal{F}_{\text{pre}}$ is named "Filter Look Up Table" (FLUT).

This configuration is represented in Fig.3.

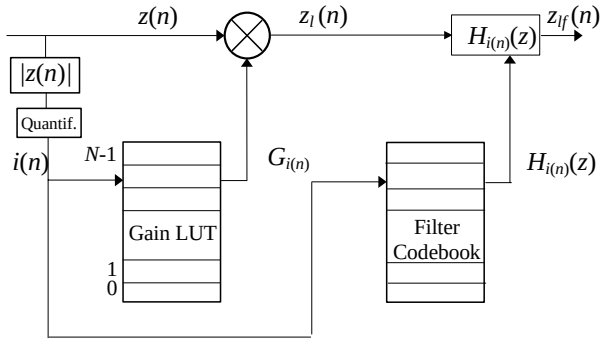

Fig. 3. Proposed FLUT predistortion system

The FLUT structure presents similarities with a Hammerstein model in which a static non-linearity (NL) is followed by a linear system (filter). The Hammerstein model uses a single filter while in the FLUT model there is a codebook of filters. The selection of the active filter in this codebook depends on the magnitude of the NL input. Therefore we can expect from our structure a gain versus input power curve whose shape depends on the frequency of a pure tone input, which corresponds to real behaviour of a non linear system with memory effects.

The LUT is filled with complex gain values. The gain applied to a signal input $z(n)$ is a complex value $G_{i(n)}$ that depends on the magnitude of $z(n)$. Cavers has studied the optimal addressing of the LUT [26] and he has shown that a uniform quantization of the input magnitude is very closed to the optimum solution. Therefore we applied this addressing technique.

For a LUT with N entries, the magnitude $|z(n)|$ is quantized uniformly on N values between 0 and a maximum value x_{max}.

If we note q the quantization step $\left(q = \frac{x_{\max}}{N-1}\right)$, the index $i(n)$ of the quantized value of the magnitude $|z(n)|$ is given by:

$$i(n) = \left\lfloor \frac{|z(n)|}{q} + \frac{1}{2} \right\rfloor, \quad (8)$$

where $\lfloor x \rfloor$ represents the integer part (floor truncated) of x.

The gain of the predistorter is the $i(n)^{th}$ value of the LUT $G_{i(n)}$.

The input and output of the LUT part of the PD are then related by:

$$z_l(n) = G_{i(n)} z(n) \quad (9)$$

The index $i(n)$ further determines which filter in the filter codebook will be applied to the LUT-distorted signal $z_l(n)$.

We use Finite Impulse Response (FIR) filters characterized, for the j^{th} filter, by their transfer function H_j and impulse response h_j related by:

$$H_j(z) = \sum_{k=0}^{L-1} h_j(k) z^{-k} \quad (10)$$

The global FLUT system is characterized by the following input-output relation, for a given input-magnitude index $i(n)$:

$$z_{lf}(n) = \sum_{k=0}^{L-1} h_{i(n)}(k) z_l(n-k) = \sum_{k=0}^{L-1} h_{i(n)}(k) G_{i(n-k)} z(n-k) \quad (11)$$

where $G_{i(n-k)}$ is the gain of the LUT corresponding to the index of the quantized value of the magnitude $|z(n-k)|$.

The global coefficient $h_{i(n)}(k) G_{i(n-k)}$ of $z(n-k)$ thus depends on the quantized magnitudes of $z(n)$ and $z(n-k)$.

The FLUT system will be further represented by the diagram of Fig. 4 and we note the index i instead of $i(n)$ to simplify the equations in the following.

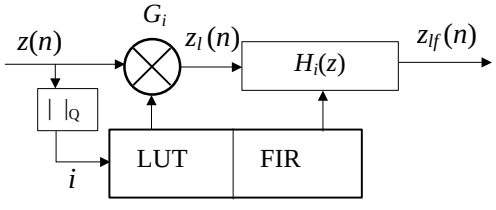

Fig. 4. Simplified representation of FLUT system

B. Proposed direct and indirect learning structure

In the FLUT system, learning (Fig. 2) is based on a combination of a direct approach for the adaptation of the gains of the LUT and an indirect approach for the adaptation of the filters coefficients.

Fig. 5.a represents the direct learning of the LUT and Fig. 5.b the indirect learning of the filter coefficients for the adaptation of the FLUT method.

1) Direct learning of LUT

It has been demonstrated that the direct learning for the adaptation of the LUT coefficients is more precise than the indirect approach [9]. We have chosen the substitution method proposed by Cavers [26] for its low-complexity and short convergence time.

At time n, according to Fig. 5(a), the normalized output of the amplifier $z_{lfa}(n)$ should be equal to the input $z(n)$. If the magnitude $|z(n)|$ determines the index i of the LUT, the i^{th} complex gain of the LUT is adapted by a substitution method. At iteration $k+1$ the new gain value $G_i^{(k+1)}$ is related to the precedent one $G_i^{(k)}$ by:

$$G_i^{(k+1)} = G_i^{(k)}\left(1-\delta\frac{z_{lfa}(n)-z(n)}{z_{lfa}(n)}\right). \quad (12)$$

where δ is an adaptation step.

2) Indirect learning of FIR filter coefficients

The indirect approach has been chosen for the adaptation of the filter coefficients because a direct minimization of a least square criterion on error $z(n)$-$z_{lfa}(n)$ would lead to a non linear equation [11].

According to this choice and Fig. 5.b we minimize a least square criterion J on the error $z_{lf}(n)$-$z_{lfalf}(n)$.

If the magnitude at the PA output $|z_{lfa}(n)|$ determines the index j of the LUT (in the postdistorter), the FLUT output $z_{lfalf}(n)$ can be written:

$$z_{lfalf}(n) = \mathbf{h}_j^{\mathrm{T}}\mathbf{z}_{\mathrm{lfal}}(n) \quad (13)$$

where:

$\mathbf{h}_j^{\mathrm{T}} = \left(h_{j,0} \quad h_{j,1} \quad \cdots \quad h_{j,L-1}\right)$ is the vector of coefficients of the j^{th} filter and:

$\mathbf{z}_{lfal}^{T}(n) = \left(z_{lfal}(n) \quad z_{lfal}(n-1) \quad \cdots \quad z_{lfal}(n-L+1)\right)$ is the vector of past samples at the output of the LUT part of the FLUT system.

The criterion $J = \sum_n \left|z_{lf}(n) - z_{lfalf}(n)\right|^2$ is a quadratic form of the filter coefficient vector $\mathbf{h}_j$.

This vector is adapted according to a LMS algorithm. At iteration $k+1$:

$$\mathbf{h}_j^{(k+1)} = \mathbf{h}_j^{(k)} + \mu\mathbf{z}_{lfal}^{*}(n)\left(z_{lf}(n) - z_{lfalf}(n)\right) \quad (14)$$

where μ is the adaptation step of the algorithm.

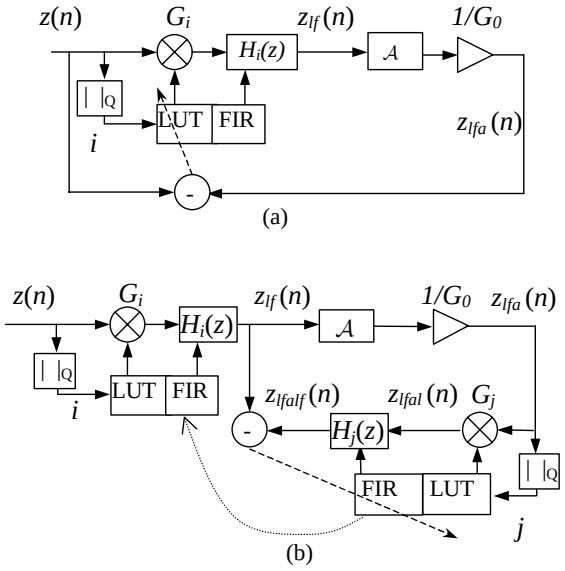

Fig. 5. Direct learning of LUT (a) and indirect learning of FIR (b) in the FLUT system

IV. Experiments and Results

We first describe the experimental conditions (model for the PA, input signal, PA operating point) and criteria of our study. Next we determine an optimal set of parameters for the FLUT method. Then we compare the FLUT performances and complexity with those of two other PD systems, namely a LUT (with direct learning) and a memory polynomial (with indirect learning). We complete this study by the analysis of the other imperfections (finite precision of converters, delay, modulator and demodulator imbalances) in the overall PD system.

A. Experimental conditions

1) Memory polynomial model for the PA

The different algorithms have been tested on a model of a class AB PA working at 1.455 GHz described in [28]. This power amplifier was built with a Motorola model MRFC1818 GaAs MESFET.

To take into account the memory effects of the PA, we used a polynomial model with memory for the PA model. The PA output at time n is given by the following equation :

$$\mathcal{A}\left(\mathbf{z}(n)\right) = \sum_{j=0}^{D}\sum_{k=1}^{P} a_{k,j}\,z(n-j)\left|z(n-j)\right|^{k-1} \quad (15)$$

with: $\mathbf{z}^{T}(n) = \left(z(n),...,z(n-D)\right)$.

The model coefficients were identified by minimizing the mean square error E between the output of the model and the measured signal $z_{out}(n)$ at the output of the PA.

$$E = \sum_n \left|\mathcal{A}\left(\mathbf{z}(n)\right) - z_{out}(n)\right|^2 \quad (16)$$

This identification was realized using real temporal signals obtained simultaneously at the input and output of the PA. These signals were provided to us by J.I. Diaz [28]. The input

signal is an OFDM type signal. The output signal is obtained using subsampling techniques.

We used P=6 (order of polynomial) and D=1 (length of memory). After the identification of the model, we have normalized the coefficients $a_{k,j}$ in order to obtain an output and an input saturation values equal to 1.

Fig. 6 represents the normalized magnitude of the PA output signal versus the m**a**gnitude of a CDMA input signal. In the following, we call "AM-AM characteristic" this type of representation giving the magnitude of the system output versus the magnitude of the input. For Fig. 6, the average input power was set to 15 dB below the saturation power of the PA. The memory effects are responsible for the thickening of the curve.

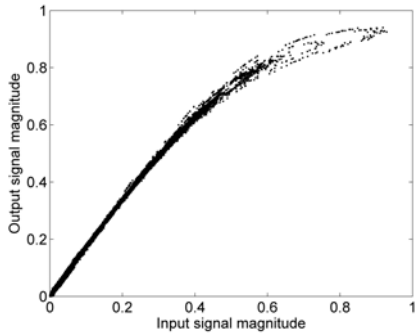

Fig. 6. AM-AM characteristic of the power amplifier

2) *Input signal characteristics and PA operating point*

a) CDMA input signal

For the test of the methods, we have used a CDMA (Code Division Multiple Access) input signal. This type of signal is proposed for many mobile communications system such as UMTS. It has many interests for mobile communications but it presents a large PAPR which results in very low efficiency for the PA when no linearization technique is used.

More precisely, the parameters of the CDMA signal are the following ones: 16 QAM symbol mapping, spreading factor equal to 32, shaping filter equal to a root raised cosine with a roll-off of 0.22, sampling rate equal to 8 times the CDMA chip rate.

The PAPR depends on the direction of the communication. For an uplink communication, the PA transmits the signal of a single user and the average PAPR is equal to 4.7 dB after the shaping filter. For a downlink communication, The PAPR depends on the number of simultaneous users sharing the same PA.

Our simulations were done with a CDMA signal corresponding to 16 simultaneous users (half load for a spreading factor of 32). This results in a PAPR of 15.2 dB (calculated on a duration of 3450 QAM Symbols) after the shaping filter. For 8 and 4 simultaneous users, the PAPR is reduced to respectively 12.3 and 9.5 dB.

b) Choice of the PA operating point

The choice of the PA operating point is very seldom discussed in publications on predistortion systems. However it is an important point in the performance evaluation of predistortion methods.

For a fair evaluation of the predistortion, we compare the performance achieved by the linearized system PD+PA with those obtained by the PA alone for the same average output power $\overline{P}^{out}$. We have to choose two different operating points, one for the linearized PA and one for the PA alone.

For the linearized system, we choose the peak backoff and the reference gain G_0. The choice of the G_0 is arbitrary and has no consequence on the performance (see Fig. 7).

Fig. 7 illustrates the power input-output relations for a PA without linearization and for the PA with an ideal PD using two different reference gains.

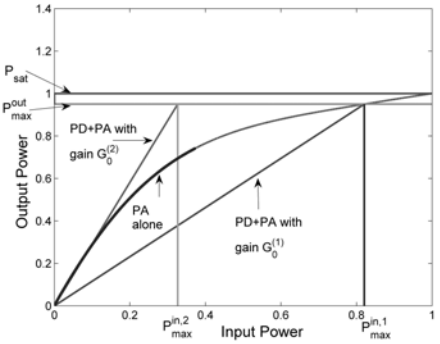

Fig. 7. Output power versus input power for 3 cases: PA without linearisation, PA with ideal PD and 2 different reference gains. Plain lines curves correspond to the same average output power.

In our experiments, we have chosen a reference gain equal to G_0 which corresponds to $G_0^{(1)}$ of Fig.7 :

$$|G_0| = \sqrt{\frac{P^{out}_{\max}}{P^{in}_{\max}}}, \tag{17}$$

with $P^{in}_{\max} = P^{in,1}_{\max}$ of Fig.7 and the average output power, after linearization, is equal to:

$$\overline{P}^{out} = |G_0|^2 \, \overline{P}^{in} = \frac{P^{out}_{\max}}{P^{in}_{\max}} \overline{P}^{in} = \frac{P^{out}_{\max}}{P^{in}_{\max} / \overline{P}^{in}}. \tag{18}$$

This can be written in decibel as:

$$\overline{P}^{out}_{dB} = P^{out}_{\max,dB} - PAPR^{in}_{dB} = P^{out}_{sat,dB} - PBO_{dB} - PAPR^{in}_{dB}. \tag{19}$$

Equation (19) explains the influence of the PBO choice: The smaller the PBO, the larger the average output power.

If we want to increase the average output power for the same PBO, we must decrease the input PAPR by clipping the input signal but this distorts the signal.

In our experiments, we have chosen a PBO equal to 0.13 dB (equivalent to a span of 0.97) and considered that the PAPR is equal to 16.2 dB (1 dB above that estimated in section IV.A.2)a)).

Because of the linear input-output relation for the linearized PA, it is easy to calculate the average output power corresponding to an input average power. For the PA without

linearization the same relation is more difficult to obtain because of the non-linear characteristic of the PA. It depends both on the PA characteristic and on the density probability function (pdf) of the input power. However, for a CDMA input signal with a sufficient number of users sharing the same transmitter, we can consider that the signal is gaussian and that the instantaneous power has a nearly decreasing exponential pdf. As the input PAPR is large, the signal amplitude is most of the time small and for these small values the PA is operating in its linear region with a gain G_{lin}. Therefore it is possible to approximate the average output power of the non-linearized PA by $|G_{lin}|^2 \bar{P}_{PA}^{in}$, where $\bar{P}_{PA}^{in}$ is the average input power of the non-linearized PA.

For a fair evaluation of the predistortion, we compare the performance achieved by the linearized system PD+PA with an average input power $\bar{P}_{PD+PA}^{in}$ with those obtained by the PA alone with an average input power $\bar{P}_{PA}^{in}$, these average input powers leading to the same output power and verifying the relations:

$$\bar{P}^{out} = |G_0|^2 \bar{P}_{PD+PA}^{in}, \tag{20}$$

and

$$\bar{P}^{out} \approx |G_{lin}|^2 \bar{P}_{PA}^{in}. \tag{21}$$

With our choice of G_0 ($<G_{lin}$), the average input power of the PD+PA system must be larger than the one of the PA without linearization in order to obtain the same average output power. They are related by:

$$\bar{P}_{PD+PA}^{in} \approx \left|\frac{G_{lin}}{G_0}\right|^2 \bar{P}_{PA}^{in}. \tag{22}$$

For the simulated amplifier the ratio G_{lin}/G_0 is equal to 1.7. Therefore, in order to obtain the same output power, the PAPR at the input of the PA without PD is fixed to 21 dB instead of 16.2 dB at the input of the system PD+PA.

3) Criteria and parameters for performance evaluation

We will present the performances of the predistortion systems according to various evaluation criteria.

The first one consists in evaluating the reduction of spectral regrowth achieved by the predistorter. Thus we examine the power spectral densities (psd) of signals and qualify the spectral regrowth by the adjacent channel power ratios (ACPR), which are calculated as the ratio of the power in the main channel and the power in the right and left adjacent channel (with no overlap between the channels).

The right and left channel ACPR are defined by:

$$ACPR_R = 10\log\left(\frac{\int_{-F_c/2}^{F_c/2} P(f)df}{\int_{F_c/2}^{3F_c/2} P(f)df}\right),$$
$$ACPR_L = 10\log\left(\frac{\int_{-F_c/2}^{F_c/2} P(f)df}{\int_{-3F_c/2}^{-F_c/2} P(f)df}\right) \tag{23}$$

where F_c represents the bandwidth of the input signal and is equal to the chip rate multiplied by the rolloff of the shaping filter.

Secondly we can evaluate the deformation of the constellation at the output of the linearized transmitter with an EVM parameter defined by (24).

$$EVM = \sqrt{\frac{\min_{\alpha,\beta}\sum_k \left|S_s(k) - \left((S_t(k)-\beta)/\alpha\right)\right|^2}{\sum_k |S_s(k)|^2}}. \tag{24}$$

In (24), $S_s(k)$ represent the original source symbols and $S_t(k)$ the actually transmitted symbols.

The parameters α and β are optimized in order to compensate for a rotation and an offset of the constellation. The EVM criterion is of fundamental importance as it is linked with the Symbol Error Rate.

It has to be noticed that this EVM definition is not the common one used in IEEE standards where EVM is measured at the receiver level, not at the transmitter one. Our definition does not take into account the transmission channel noise and distortions but focuses on the PA distortions.

To study the convergence of algorithms we are also interested in the decrease of the instantaneous squared error between the input signal and the normalized predistorted-amplified signal. As the error $z(n)$-$z_{pa}(n)$ itself exhibits large and fast variations we will present smoothed curves obtained by a sliding average of the squared errors.

The AM-AM curves obtained with and without predistortion will demonstrate the accuracy of the methods to linearize the PA and to reduce memory effects by thinning the curves.

B. Choice of FLUT parameters

1) LUT size

We have studied the influence of the LUT size N on the performance. We have tested N = 8, 16, 32, 64 and 128 with corresponding filters of length L=8 (10) .

As shown in Fig. 8 the ACPR values increase with the LUT size N until it reaches N=64.

Table I gathers the corresponding EVM and demonstrates that N=64 is the best choice for the LUT size parameter.

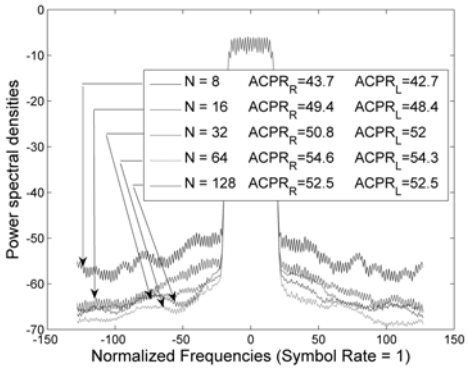

Fig. 8. Power spectral densities and ACPR at the output of the FLUT system for different values N of the LUT size.

The value N = 64 has been used in the following.

TABLE I
EVM FOR DIFFERENT VALUES OF THE LUT SIZE

LUT size (N)	8	16	32	64	128
EVM(%)	0.74	0.42	0.23	0.21	0.26

2) FIR length

We have tested several lengths for the FIR filters of the FLUT predistorter.

TABLE II
EVM AND ACPR FOR DIFFERENT LENGTHS OF FIR

L (FIR length)	FLUT	
	ACPR (dB)	EVM(%)
0	48	1.41
2	51.8	0.27
4	53.9	0.22
8	54.5	0.21

Table II gives the values of average ACPR and EVM obtained with a LUT of size N= 64 (no filters) and three FLUT systems with $N = 64$ and $L = 2, 4, 8$. The average ACPR is the average of ACPR right and left and the average EVM is the average calculated on the 16 users.

According to this table we can see that a FLUT PD with a codebook of 2-coefficients filters achieves a gain of more than 3 dB of ACPR over a simple LUT. We further observe that with increasing length of filter the spectral regrowth is reduced up to 6 dB.

In terms of EVM, the three cases achieve similar results (~0.25%) which are clearly better than the value obtained with a simple LUT (~1.4%).

However for L=16 the performances decrease (they are close to those obtained with L=2). In the following we consider L=8.

3) Adaptation step

We have tested different adaptation steps μ (14) for the learning of FIR coefficients of the FLUT. We used $\mu=0.5$, which has demonstrated to be the optimal value for different lengths of filters, in the following.

The adaptation step δ (12) for the LUT was set to 0.1 in all the experiments.

4) Initialization of the FLUT predistorter

We start with a "transparent" predistorter, i.e. the LUT is initialized with values equal to one and the impulse responses of the FIR filters are unit impulses. With this initialization, the output of the PD is equal to its input.

C. Comparison with two reference methods

1) Reference Predistorters

In order to evaluate the FLUT system performances we have compared it with two reference predistortion systems:

- an N entry LUT adapted through a direct learning according to the Cavers's algorithm presented in III B 1. We will refer to this method as the LUT method

- a memory polynomial predistorter. The input-output relation of a memory polynomial PD is described by the following equation:

$$\mathcal{F}\left(\mathbf{z}(n)\right)=\sum_{k=1}^{P}\sum_{j=0}^{D} f_{k,j}\, z(n-j)\left|z(n-j)\right|^{k-1}=\mathbf{f}^{\mathrm{T}}\mathbf{v}_n \qquad (25)$$

with: $\mathbf{f}=\left(f_{1,0},...,f_{P,0},...,f_{1,D},...,f_{P,D}\right)^{\mathrm{T}}$,

and: $\mathrm{v}_n =$

$$\left(z(n),...,z(n)\left|z(n)\right|^{P-1},...,z(n-D),...,z(n-D)\left|z(n-D)\right|^{P-1}\right)^{\mathbf{T}}.$$

This system is adapted through an indirect learning using a Recursive Least Square (RLS) algorithm which updates the coefficient vector **f** (of length $P(D+1)=O$) by minimizing the criterion:

$$J=\sum_{l=P}^{n}\left|\mathcal{F}\left(\mathbf{z}_{pa}(l)\right)-z_p(l)\right|^2. \qquad (26)$$

We have set the parameters of this method to: order $P = 6$ and delay $D = 1$. We will refer to this method as MEM-POLY [15].

2) Comparison of performances

We have compared the FLUT method (N=64, L=8) with the LUT method (N=64) and the MEM-POLY method in terms of power spectral densities, ACPR, errors, constellations, EVM, AM-AM curves and linearization.

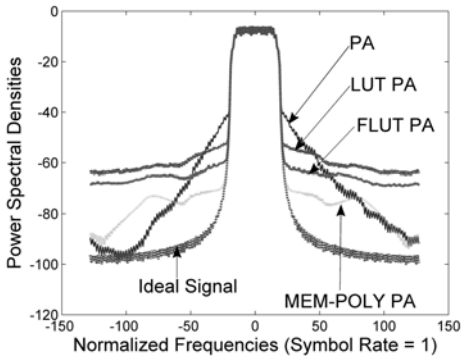

Fig. 9. psd of PA output signals for different methods of predistortion

As demonstrated in Fig.9 the psd obtained with the FLUT method lies between those obtained with the LUT and the MEM-POLY methods.

Fig. 10 plots the constellations (16 QAM) of received symbols after demodulation of the signals (at the output of PA). We only show the cases of the simple LUT predistorter and of the FLUT predistorter because it is not possible to distinguish the "ideal" constellations from the true received ones as soon as the EVM is low enough (<0.5%) which is the case for both MEM-POLY and FLUT predistorters.

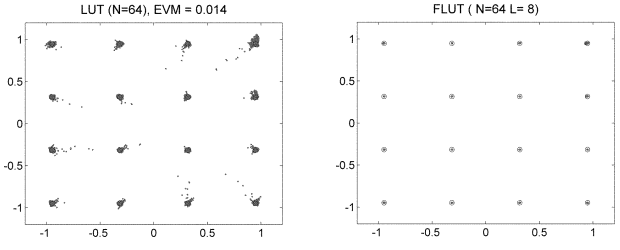

(a) (b)

Fig. 10. Constellations of received symbols for different methods of predistortion: (a) LUT method, (b) FLUT method.

According to this Fig.10, the simple LUT method doesn't achieve sufficient compensation of the PA effects.

The smoothed squared errors are plotted on Fig.11.

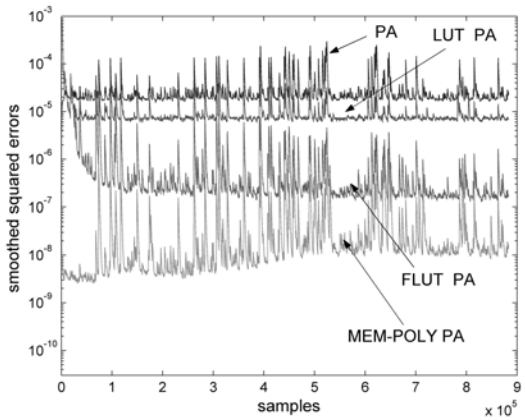

Fig. 11. Smoothed quadratic errors between complex envelops of input and output of PD-PA systems for different methods of predistortion

For the FLUT method, the learning of the predistorter starts with a first stage (~100 CDMA symbols) during which only the LUT is adapted. The adaptation of the FIR coefficients is started after this stage (while the adaptation of LUT is going on), which explains a slower convergence of that method compared with MEM-POLY. After convergence the smoothed squared error resulting from the FLUT method lies between those resulting from LUT and MEM-POLY methods.

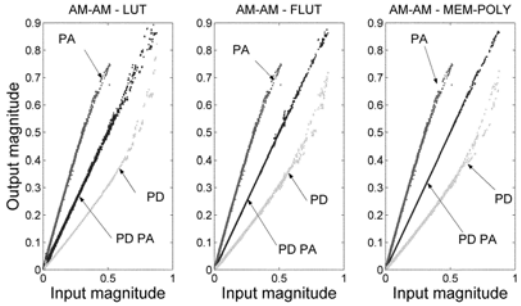

Fig. 12. AM-AM curves for different methods of predistortion

Fig. 12 represents the AM-AM curves of the following signals:

- amplified signal versus input signal without predistortion,
- predistorted signal versus input signal,
- predistorted and amplified signal versus input signal

for each of the three studied methods (LUT, FLUT and MEM-POLY).

The memory effects are not taken into account in the LUT method. Thus the predistorted AM-AM curve is thinner for the predistorted signal of the LUT method, which results in a thicker predistorted and amplified curve.

TABLE III
EVM AND ACPR FOR DIFFERENT METHODS OF PREDISTORTION

	ACPR (dB)	EVM(%)
PA output without PD	44.4	2.77
LUT	48	1.41
FLUT	54.4	0.21
MEM-POLY	63.7	0.08
Reference signal	76.8	0

Table III gathers the EVM and ACPR of the three methods. We can notice that these quantitative results are in accordance with the preceding qualitative performances.

3) Comparison of complexity

The complexity is evaluated by counting the number of elementary operations (addition, multiplication, division) per input sample. These operations may be real or complex. Therefore in order to unify the counts, we have converted complex operations in equivalent real operations. For each complex multiplication, 4 real multiplications and 2 additions are counted, one complex addition needs 2 real additions and a reciprocal of a complex number (used to calculate a division) is evaluated as 4 real multiplications, 1 addition and 1 real reciprocal.

The table readings or writings are neglected.

For the three compared methods it is necessary to calculate the square root of the signal magnitude. This operation is not taken into account in our estimation of the complexity because it is common to the three methods and there are different ways of calculating a square root.

a) LUT method

Table IV gives the complexity of the LUT method, for a LUT with N entries.

The complexity of the LUT method does not depend on the size of the LUT. It is equal to 31 real additions or multiplications plus 2 real divisions per sample.

TABLE IV
COMPLEXITY OF THE LUT METHOD

Tasks	real add	real mult.	real div.
LUT address	1	2	1
LUT gain	2	4	
LUT update	8	14	1
Total	11	20	2

b) FLUT method

Table V gives the complexity of the FLUT method, for a LUT with *N* entries and FIR filters with *L* coefficients. The total number of real elementary operations is equal to 8*L*+31 additions or multiplications and 2 divisions par sample.

TABLE V
COMPLEXITY OF THE FLUT METHOD

Tasks	real add.	real mult.	Real div.
LUT address	1	2	1
LUT gain	2	4	
LUT update	8	14	1
Filtering	$2(L-1)$	$2L$	
Filter update	$2L$	$2(L+1)$	
Total	$4L+9$	$4L+22$	2

Numerical Application: For FIR filters of length L=8, the complexity of the FLUT method is equal to 8L+31=95 real additions or multiplications plus 2 real divisions, which is approximately 3 times more than the LUT method.

c) MEM-POLY method

In the MEM-POLY method, the predistortion system is defined by the relation given in (25) presented in section IV.C.1).

The RLS algorithm, which updates the coefficient vector $\mathbf{f}$ (of length $P(D+1)=O$) requires the following steps:

- Updating of Kalman gain $\mathbf{K}$:

$$\mathbf{K} = \mathbf{K} - \frac{\mathbf{K}\mathbf{v}_n^* \mathbf{v}_n^T \mathbf{K}}{1+\mathbf{v}_n^T \mathbf{K}\mathbf{v}_n^*}, \quad (27)$$

where vector $\mathbf{v}_n$ was defined in (25),

- Updating of coefficient vector $\mathbf{f}$:

$$\mathbf{f} = \mathbf{f} + \mathbf{K}\mathbf{v}_n^* (z_p - \mathbf{v}_n^T \mathbf{f}). \quad (28)$$

The predistortion itself is implemented according to (25).

Table VI gives the number of elementary operations for each task. The total number of real elementary operations is equal to $22O^2+26O-4D-8$ real additions or multiplications plus 1 division per sample.

TABLE VI
COMPLEXITY OF THE MEM-POLY METHOD

Tasks	real add.	real mul.	real div.
Formation of $\mathbf{v}$		$2O-2(D+1)$	
$\mathbf{K}$ update	$6O^2-2O+2$	$16O^2+4O-4$	1
$\mathbf{f}$ update	$4O$	$8O$	
Predistortion	$4O-2$	$6O-2(D+1)$	
Total	$6O^2+6O$	$16O^2+20O-4D-8$	1

Numerical Application: For $D = 1$ and $P = 6$, the parameter O is equal to 12 and the complexity of the MEM-POLY method is equal to 3468 real additions or multiplications plus 1 real division per sample which is approximately 36 times that of the FLUT method and 112 times that of the LUT method.

The complexity of the MEM-POLY technique is considerably higher than those of the FLUT or simple LUT methods. It is of an order of magnitude higher than the FLUT method.

D. Influence and compensation of imperfections

We have evaluated by simulation the FLUT technique in the presence of different imperfections of the components of the overall predistortion system (Fig.1) : finite precision of DAC and ADC, loop delay, quadrature modulator and demodulator imbalances. We have verified that the imperfections due to the loop delay and to the quadrature (de)modulator can be compensated.

1) Quantization effects

We have tested the FLUT approach with different numbers of bits (8, 10, 12, 14) for the DAC and ADC Converter respectively. In each experiment, the number of bits of one type of converters (DAC or ADC) is fixed to 14 and the number of bit of the other type is changed from 8 to 14 with a step equal to 2.

Table VII gives the values of average ACPR and EVM for the different tests.

TABLE VII
ACPR AND EVM FOR DIFFERENT NUMBER OF BITS OF DAC AND ADC

Number of bits DAC	average ACPR	EVM in %
8	34.1	1.3
10	45.3	0.39
12	52.2	0.27
14	53.4	0.26

Number of bits ADC	average ACPR	EVM in %
8	46.7	0.43
10	50.6	0.30
12	53.3	0.26
14	53.4	0.26

We can observe that a precision of 12 bits on the DAC is necessary. Otherwise we lose the benefits of the PD device (see table III).

It can be noticed that the requirement on the ADC precision is less severe than those on the DAC which can be explained by the fact that the ADC has no direct influence on the output signal as it is only responsible of the precision on the feedback path which controls the adaptation of the PD device. A precision of 10 bits on the ADC appears acceptable.

2) Loop delay

The analog devices present in the forward transmission path or feedback path of the emitter, in particular the PA, introduce delays which generate a time mismatch between the modulated signal $z(t)$ and the PA demodulated signal $z_{pa}(t)$. This loop delay τ is very harmful and has to be compensated.

Table VIII illustrates the influence of a delay on the average ACPR and the EVM for different values of the delay expressed in percent of the sampling period T_S. For $\tau / T_S <$ 20%, we can notice that the EVM increases linearly with the delay and that the ACPR looses 2 dB when the delay is

increased by 5% percent of T_S. For τ / T_S > 20%, the results become worse very fast.

TABLE VIII
ACPR AND EVM FOR DIFFERENT VALUES OF THE LOOP DELAY

Delay in % of the sampling period	ACPR (dB)	EVM(%)
0	54.5	0.21
2	52.5	0.34
5	51.9	0.76
10	49.9	1.5
20	45.8	3

We have applied a two-step technique for the estimation and compensation of the loop delay. During the first step, the delay is estimated. During the second step, the delay is introduced on the modulated signal and The FLUT predistorter is adapted.

Different methods for the estimation of the delay have been proposed in the literature [31], [32], [33]. For example, the ramp technique used in the TETRA standard [31] gives very good results but requires a ramp training sequence. With the TETRA technique, we obtained a precision better than 2% of T_S.

The compensation of the loop delay τ is realized by delaying the modulated signal of the same value. The ratio τ / T_S is the sum of an integer part and a fractional part. We have implemented the fractional delay by a 4-coefficient FIR filter with the Farrow structure [34].

3) Quadrature Modulator impairments

We have studied the influence of the Quadrature Modulator (QM) imperfections (gain and phase imbalances, DC offsets) on the performances of the transmitter chain.

If the complex envelop at the output of the predistortion device is $z_p=I+jQ$, the complex envelop of the modulated signal is given by:

$$z_M = \left(\alpha_M \left(I + c_{MI}\right) + \beta_M \left(Q + c_{MQ}\right)\sin\left(\phi_M\right)\right) + j\left(\beta_M \left(Q + c_{MQ}\right)\cos\left(\phi_M\right)\right) \quad (29)$$

With:

- DC offset errors: c_{MI} and c_{MQ} on I (in-phase) and Q (in- quadrature) components of the signal respectively (due to both the quadrature modulator and DA converters preceding the QM)
- Amplitude gains in the I and Q branches: α_M and β_M respectively.
- Phase shift error: ϕ_M (i.e. deviation from the optimal value $\pi/2$ of the phase shift between the two quadrature carriers).

The gain imbalance can be characterized by $\varepsilon_M = \frac{\alpha_M}{\beta_M} - 1$.

We have inserted these QM defaults between the predistortion and the PA models with the following (typical) values:

$\varepsilon_M=0.1$, $\phi_M=1°$, $c_{MI}=-c_{MQ}=0.01x\ A_{max}$ where A_{max} is the maximum magnitude input value.

Without any compensation, the effects of these imperfections in the PD-PA chain are dramatic: ACPR is only 11 dB and EVM reaches 33%. This is quite understandable if we keep in mind that in our simulations we start with a "transparent" predistorter and we adapt it at each sample with a criterion which is biased in case of QM imbalances. The worst imperfection is the introduction of offsets without which the EVM is only 4% and the ACPR 39 dB.

Cavers [30] has proposed a technique to deal with these modulator imbalances. The idea consists in introducing a QM compensator (QMC) in front of the DAC which guarantees a transparent QMC-QM system. The implementation of this technique leads to results very close to those obtained without any imperfections: ACPR = 54 dB (instead of 54.5 dB) and EVM = 0.26% (instead of 0.21%).

4) Quadrature Demodulator impairments

We have studied the influence of Quadrature Demodulator (QDM) imperfections (gain and phase imbalances, DC offset) and we proposed a new algorithm for the compensation of these imperfections which is derived from that proposed by Cavers [30] for the QM.

The implementation of this technique of compensation leads to results analog to those obtained without any imperfections.

When we compensate for imperfections of typical values introduced in both of the Quadrature Modulator and Quadrature Demodulator we get performances close to original ones: EVM=0.25% and ACPR=53.4 dB.

V. CONCLUSION

We have proposed a new adaptive baseband predistortion method for the linearization of Power Amplifiers (PA) exhibiting memory effects. It is based on a LUT associated to a codebook of FIR filters addressed by the index of the LUT.

We have tested this method in the presence of imperfections such as finite precision of ADC and DAC, quadrature modulator and demodulator defects and loop delay. We have shown that the imperfections due to the loop delay and to the quadrature modulator and demodulator can be compensated. We have proposed an adaptive algorithm to correct the imperfections of the quadrature demodulator derived from that proposed by Cavers [30] for the quadrature modulator.

We have compared this FLUT method with two other approaches: a simple LUT with substitution adaptation method and a memory-polynomial predistorter with indirect learning by RLS algorithm.

The FLUT method achieves performances that lie between those of a simple LUT and those of a memory polynomial system.

The LUT method is the less complex and is currently used in commercial predistortion devices [29]. Its performance is however limited in presence of PA memory effects.

The complexity of the memory polynomial method grows as the square power of the coefficient vector length. The

updating of this vector uses most of the computational load. Therefore, this method does not appear at the present time as a practical solution for wideband applications.

The complexity of the FLUT method is one order of magnitude smaller than the complexity of the memory polynomial. It grows linearly with the length of FIR filters. This method can be implemented on Digital Signal Processors for mobile communication systems even for wideband signals. Compared with the LUT method, the addition of a codebook of filters in the FLUT predistorter adds the possibility to compensate for memory effects.

ACKNOWLEDGMENT

The authors are grateful to J.I. Diaz for providing the real temporal signals allowing the modeling of the power amplifier.

REFERENCES

[1] S.C. Cripps, *RF Power Amplifiers for wireless communications.* Norwood, MA: Artech House, 1999.

[2] J. Vuolevi, T. Rahkonen, J. Manninen, "Measurement Technique for Characterizing Memory Effects in RF Power Amplifiers", *IEEE Trans. on Microwave Theory and Techniques*, 49(8): 1383-1389, Aug. 2001.

[3] P.B. Kennington, *High linearity RF Amplifiers design*, Artech House 2000.

[4] Y. Nagata, "Linear Amplification technique for Digital Mobile Communication", *IEEE Vehicular Technology Conf.*, San Fransisco, pp 159-164, May 1989.

[5] A. Bateman, D. M. Hainesa and R. J. Wilkinson, "Linear transceiver architectures", *Proceedings of the 38th IEEE Vehicular Technology Conference*, pp. 478-484, May 1988.

[6] M. Faulkner, T. Mattsson, W. Yates, "Adaptive linearisation using pre-distortion", *IEEE 40th Vehicular Technology Conference*, pp. 35-40, 1990.

[7] M. Faulkner, M. Johansson, "Adaptive Linearization Using Predistortion. Experimental Results", *IEEE Transactions on Vehicular Technology*, vol. 43, n.2, pp. 323-332 May 1994.

[8] J.K. Cavers, "Amplifier linearization using a digital predistorter with fast adaptation and low memory requirements", *IEEE Trans. Vehicular Tech.*, vol. 39, no.4, pp 374-382, Nov. 1990.

[9] G. Baudoin, R. Marsalek, P. Jardin "A New Approach for LUT-based Digital Predistorters Adaption", Electronic Devices and Systems Conference, Sept. 2003.

[10] A. N. D'Andrea, V. Lottici, R. Reggiannini, "RF power amplifier linearization through amplitude and phase predistortion", *IEEE transactions on communications*, vol. 44, no. 11,pp. 1477-1484, Nov. 1996.

[11] R. Marsalek, P. Jardin and G. Baudoin, "From post-distortion to predistortion for power amplifiers linearization", *IEEE Communication Letters*, vol. 7, July 2003.

[12] J. Kim, K. Constantinou, "Digital predistortion of wide band signals based on power amplifier model with memory", *Electronic Letters*, vol. 37, no. 23, pp. 1417-1418, nov 2001.

[13] C. R. Giardina, J. Kim, K. Konstantinou, "System and method for predistorting a signal based on current and past signal samples", US patent application 09/915042, July 2001.

[14] L. Ding, G. T. Zhou, D. R.Morgan, Z. Ma, J. S. Kenney, J. Kim, C. R. Giardina, "A robust digital baseband predistorter constructed using memory polynomials", *IEEE Transactions on Communications*, Vol. 52, Issue:1, pp. 159-165, Jan. 2004.

[15] G. Baudoin, P. Jardin, R. Marsalek**,** "Power amplifier linearisation using predistortion with memory", *13th International Czech - Slovak Scientific Conference RADIOELEKTRONIKA'2003*, pp. 193-196, 6 - 7 Mai 2003 Brno, Czech Republic.

[16] Nizamuddin, M.A.; Balister, P.J.; Tranter, W.H.; Reed, J.H., "Nonlinear tapped delay line digital predistorter for power amplifiers with memory", *Proc. IEEE Wireless Communications and Networking Conference WCNC 2003* , Vol 1 , Pages:607 – 611, March 2003.

[17] C. Eun, E. J. Powers, ``A new Volterra predistorter based on the indirect learning architecture," *IEEE Trans. Signal Processing*, vol. 45, pp. 223-227, Jan. 1997.

[18] A. Zhu, T. J.~Brasil, "An adaptive Volterra Predistorter for the linearization of RF High Power Amplifiers", *Proc. Conference IEEE MTT* pp. 461-464, 2002.

[19] Lei Ding; Raich, R.; Zhou, G.T."A Hammerstein predistortion linearization design based on the indirect learning architecture", *Proc. International IEEE Conference on Acoustics, Speech, and Signal Processing, ICASSP '02.* Vol 3 , Pages:III-2689 - III-2692, May 2002.

[20] Hyun Woo Kang; Yong Soo Cho; Dae Hee Youn; "On compensating nonlinear distortions of an OFDM system using an efficient adaptive predistorter", *IEEE Transactions on Communications* , Vol 47 , Issue: 4 , Pages:522 – 526, April 1999.

[21] N. Benvenuto, F. Piazza, A. Uncini, "A neural network approach to data predistortion with memory in digital radio systems",, *IEEE International Conference on Communications ICC 93*, Vol 1 , pp. 232 - 236, Geneva, May 1993.

[22] Y. Ding, H. Ohmori and A. Sano, "Adaptive Predistortion for High Power Amplifier with Linear Dynamics," IEEE Int. MidWest Symp. on Circuits and Sys., pp.121-124, Japan, July 2004.

[23] T. Wang and J. Ilow, "Compensation of Nonlinear Distortions with Memory Effects in Digital Transmitters," IEEE Conf. On Comm. Networks and Services Research (CNSR'04), pp. 3-9, Canada, May 2004.

[24] P. L. Gilabert, G. Montoro and E. Bertran, "On the Wiener and Hammerstein Models for Power Amplifier Predistortion," Asia-Pacific Microwave Conference, APMC-05, vol. 2, pp.1191-1194, 4-7 December, Suzhou, China, 2005.

[25] T. Liu, S. Boumaiza and F. M. Ghannouchi, "Deembedding Static Nonlinearities and Accurately Identifying and Modeling Memory Effects in Wide-Band RF Transmitters," IEEE Trans. on Microwave Theory and Tech., vol 53, pp. 3578-3587. November 2005.

[26] J.K. Cavers, "Optimum table spacing in predistorting amplifier linearizers", *IEEE trans. On vehicular technology*, Vol. 48, N°5, Sept. 1999, pp. 1699-1705.

[27] J.K. Cavers, « The effect of quadrature Modulator and demodulator errors on adaptive digital predistorters for amplifier linearization », *IEEE trans. on Vehicular technology*, VoL.46, N°2, May 1997, pp. 456-466.

[28] J.I. Diaz, C. Pantaleon, I. Santamaria, "Nonlinearity Estimation in Power Amplifiers Based on Subsampled Temporal Data", *IEEE Transactions on Instrument and Measurement*, vol. 50, No.4, August 2001.

[29] Intersil Corporation, "Operation and performance of the ISL5239 Predistortion Linearizer", *Intersil application note N°AN1022*, July 2002. http://www.intersil.com/data/an/AN1022.pdf.

[30] James K. Cavers, "New methods for Adaptation of Quadrature Modulators and Demodulators in Amplifier Linearization Circuits", *IEEE Transactions on vehicular Technology*, vol. 46,no. 3, august 1997.

[31] J. de Mingo, A. Valdovinos, "Performance of a New Digital Baseband Predistorter Using Calibration Memory", *IEEE Transactions on Vehicular Technology*, vol. 50, No. 4, July 2000, pp. 1169-1176.

[32] D. Kim, S. Lee, "Analysis and Design of an Adaptive Polynomial Predistorter with the Loop Delay Estimator", *Microwave and Optical technology Letters*, Vo. 34, No. 2, July 2002, pp. 117-121.

[33] Jeckeln et al., "Adaptive Digital Predistortion for Power Amplifiers with Real Time Modeling of Memoryless Complex Gains", *US Patent* No. 6,072,364, Jun. 6, 2002.

[34] L. Erup, F.M. Gardner, R.A.Harris : "Interpolation in digital modems – part II: implementation and performance", *IEEE Trans. On Communications*, vol. 41. no. 6, June 1992.

Pascale Jardin was born in Paris, France in 1959. She received the acoustic master degree from the University of Le Mans, France in 1982 and the PhD degree from the University Paris-VI in 1984. In 1985, she joined the Department of Telecommunication and Signal Processing at the ESIEE (engineers school) France, where she is currently Associate Professor. Her past and present research interests include digital signal processing, nonlinear modeling , speech and acoustic signal processing.

Geneviève Baudoin was born in France in 1954. She graduated from the École Nationale supérieure des Télécommunications (ENST), Paris, France, in 1977 and received the Habilitation for PHD direction from the university of Marne La Vallée in 2000.
She was lecturer at the university of Paris-Ouest; then she joined the Philips Research laboratory in France, as a research-engineer.
Since 1981, she has been with the École Supérieure d'Ingénieurs en Électronique et Électrotechnique de Paris (ESIEE). She is presently Professor with the department of Telecommunications and Signal Processing and Research Director at ESIEE. Her research and teaching activities include wireless communications, digital signal processing and speech processing.